Impact of black phosphorus nanosheet exposure on growth, reproduction, antioxidant mechanisms, and transcriptomic responses in Daphnia magna

Luo, T.; Zhang, P.; Wang, J.; Shi, J.; Di, Y.; Liu, G.; Peijnenburg, W.J.G.M.

Aquatic Toxicology 283 (2025) 107333

Contents lists available at ScienceDirect

Aquatic Toxicology

journal homepage: www.elsevier.com/locate/aqtox

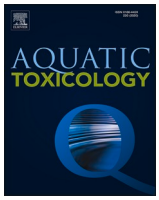

Impact of black phosphorus nanosheet exposure on growth, reproduction, antioxidant mechanisms, and transcriptomic responses in *Daphnia magna*

Tianlie Luo [a,b,c], Ping Zhang [a,b,c], Jinyu Wang [a,b,c], Jingjing Shi [a,b,c], Yubo Di [a,b,c], Guo Liu [a,b,c,*], Willie J.G.M. Peijnenburg [d,e]

[a] State Key Laboratory of Geohazard Prevention and Geoenvironment Protection, Chengdu University of Technology, Chengdu 610059, China
[b] State Environmental Protection Key Laboratory of Synergetic Control and Joint Remediation for Soil & Water Pollution, Chengdu University of Technology, Chengdu 610059, China
[c] College of Ecology and Environment, Chengdu University of Technology, Chengdu 610059, China
[d] Institute of Environmental Sciences (CML), Leiden University, Leiden, 2300, RA, the Netherlands
[e] National Institute of Public Health and the Environment, Centre for the Safety of Substances and Products, Bilthoven, 3720, BA, the Netherlands

ARTICLE INFO

Keywords:
Black phosphorus nanosheets
Daphnia magna
Chronic toxicity
Transcriptomics
Growth reproduction

ABSTRACT

Black phosphorus nanosheets (BPNS), a novel two-dimensional nanomaterial, have garnered significant attention in biomedical and technological applications due to their exceptional physicochemical properties. However, their widespread use raises concerns about potential environmental risks. In this study, we elucidate the toxicological mechanisms of BPNS on *Daphnia magna* (*D. magna*), a model aquatic organism. The results reveal that BPNS is efficiently absorbed and accumulates in the intestinal tract of *D. magna*. Exposure to low concentrations of BPNS significantly alters developmental and reproductive performance, as evidenced by a 2-day acceleration in the time to first brood and an increase in body length from 3.1 to 3.3 mm. Furthermore, BPNS exposure induces oxidative stress in *D. magna*, characterized by elevated reactive oxygen species (ROS) levels, enhanced activities of superoxide dismutase (SOD) and catalase (CAT), and increased malondialdehyde (MDA) concentrations. RNA sequencing analysis indicates that dysregulation of iron homeostasis plays a pivotal role in mediating oxidative stress in *D. magna*. Concurrently, detoxification mechanisms are activated, as evidenced by upregulation of genes associated with chitin and carbohydrate metabolism, as well as cuticle structure components. Additionally, BPNS exposure modulates key signaling pathways, including the lysosomal pathway, starch and sucrose metabolism, and steroid biosynthesis, which collectively enhance the stress tolerance of *D. magna*. These findings provide critical insights into the ecological implications of BPNS release into aquatic ecosystems, highlighting the need for comprehensive risk assessments of emerging nanomaterials.

1. Introduction

Black phosphorus nanosheets (BPNS) are emerging two-dimensional nanomaterials with a puckered honeycomb layers of phosphorus atoms. Unlike conventional nanomaterials, BPNS exhibit tunable band gap, anisotropy and high carrier mobility, making them promising for applications in energy technology, biomedicine, optoelectronic devices, and biosensing (Bigham et al., 2024; Smith et al., 2024; Xu et al., 2020; Zhao et al., 2022). However, their widespread use raises concern about environment release and pose potential risks to ecosystems and human health.

Previous studies have revealed that BPNS can induce reactive oxygen species (ROS) production and is cytotoxic to mammalian cell lines such as NIH 3T3 (mouse embryo), HcoEpiC (human colon), and 293T cells (human kidney)(Qiu et al., 2018; Zhang et al., 2017). BPNS can cause nephrotoxicity through the IRE1α signaling pathway(Deng et al., 2024; He et al., 2020). BP quantum dots (BPQDs) can trigger inflammatory responses after being injected into mice, and accordingly regulate immune responses(Sun et al., 2020). Moreover, BPQDs induced inflammation, oxidative stress and apoptosis in the gut and brain tissues of zebrafish(Cao et al., 2024). Black phosphorus (BP) disrupts vascular endothelial growth factor and MAPK pathways in zebrafish, leading to abnormal cardiovascular development (Yang et al., 2021). In *Chlamydomonas reinhardtii,* BP-induced cell wall aberrations elevate ROS

* Corresponding author.
E-mail address: liuguo@cdut.edu.cn (G. Liu).

https://doi.org/10.1016/j.aquatox.2025.107333
Received 3 February 2025; Received in revised form 16 March 2025; Accepted 19 March 2025
Available online 24 March 2025

formation, causing extensive transcriptome remodeling (Chaloupsky et al., 2024).

It is noteworthy that BPNS's susceptibility to oxidation generates phosphate ions (PO_x) and dissolved phosphorus (DP), which contribute to toxicity in aquatic organism (Thurakkal and Zhang., 2020). Studies have shown that BPNS degrade rapidly in water, with a 73 % degradation rate within 8 days(Qin et al., 2020). BPNS degradation products such as phosphate ions, perturb growth in *C. vulgaris*(Li et al., 2020). However, the specific contributions of solid BP and intracellular degraded phosphorus acid remain unclear due to methodological limitations (Wu et al., 2020). Therefore, it is more critical to study the aquatic toxicity of BPNS itself.

D. magna, a small freshwater crustacean, is widely employed in ecotoxicological studies due to its sensitivity to pollutants, short growth cycle, and transparent body (Ni et al., 2025; Yang et al., 2017). Studies have shown that exposure to nanomaterials (e.g., TiO_2, AgNPs, and graphene oxide) induces complex and diverse toxic effects in *D. magna*, including oxidative stress(Lu et al., 2021) and inhibition of growth and reproduction(Wang et al., 2019). This leads to cellular oedema(Xiang et al., 2024a), and disruption of the feeding behavior of *D. magna*. Considering that BPNS are widely used and may be continuously released into the environment, it is necessary to reveal the molecular mechanisms underlying the long-term effects of BPNS on *D. magna*.

Current aquatic toxicity studies on nanomaterials have the primary objective of describing effects on conventional toxicological endpoints such as survival, behavioral changes and hatchability. However, these data do not provide critical information on the toxicity of nanomaterials. RNA sequencing technology is characterized by accurate quantification and a wide detection range, which allows for the differentiation of toxic effects of pollutants and the assessment of their mechanisms based on a comprehensive examination of biological responses. The developmental cardiotoxicity of 2-aminobenzothiazole in *D. magna* has been reported to be due to oxidative damage to the heart caused by ferroptosis, leading to oxygen supply disruption(Chen et al., 2024). Similarly, $Ti_3C_2T_x$ can lead to metabolic disturbances in *D. magna* by interfering with lipid and amino acid metabolic pathways(Xiang et al., 2024b). In addition, transcriptome analyses revealed that the toxicity of antimony trioxide nanoparticle to *D. magna* results from the combination of oxidative stress and nutrient depletion(Gu et al., 2022). Thus, transcriptomic analysis is crucial for elucidating the molecular mechanisms of BPNS toxicity in *D. magna*.

In summary, the environmental risks associated with the widespread use of BPNS have drawn significant attention. However, toxicological studies of BPNS on invertebrates remain underdeveloped, and the underlying molecular mechanisms are still unclear. In this study, *D. magna* was exposed to BPNS and the environmental hazards of BPNS to aquatic organisms were assessed by acute toxicity test and measurement of enzyme activity concentration. Then, the chronic toxicity of BPNS was determined by exposing *D. magna* to BPNS for 21d and measuring changes in calving rate, chest beat frequency, and body length. In addition, transcriptomic analyses were performed to investigate the mechanisms of toxicity. This study aims to provide a comprehensive understanding of the toxic effects and molecular mechanisms of BPNS on *D. magna*, and the results will contribute to our further understanding of the ecological risks of BPNS in the environment.

2. Materials and methods

2.1. Materials

A BPNS dispersion (200 mg/L) was purchased from XFNANO Tech Co., Ltd. (Nanjing, China) and stored in dark oxygen-free conditions before the start of the experiments (see Text S1 for details). Liquid nitrogen (99.99 %) was purchased from Chengdu Kelon Chemical Reagent Factory. The TRIzol kit was purchased from Thermo Fisher Technologies. RNase-free DNase I was purchased from Beijing Wokawei Biotechnology Co., LTD. NEBNext® Ultra™ RNA Library Prep Kit for Illumina® was purchased from Beijing NEB Co., LTD. USER Enzyme was acquired from Shanghai Qiming Biotechnology Co., LTD.

2.2. Characterization of BPNS

The BPNS suspensions were ultrasonically dispersed using a liquid crystal ultrasonic cleaner (KS-5200DE, Kunshanjielimei, China) for 5 min at 400 W before use. The morphology of the BPNS was examined by AFM (BRUKER Dimension Icon), by SEM (HITACHI, SU5000+ Oxford Instruments Ultim Max), and by TEM (FEI Tecnai G2 F20). The hydrodynamic diameter and zeta potential of BPNS in the test water ($CaCl_2{\cdot}2H_2O$ 294 mg/L, $MgSO_4{\cdot}7H_2O$ 23.3 mg/L, $NaHCO_3$ 64.8 mg/L, KCL 5.8 mg/L, pH 7.8 ± 0.2 and the dissolved oxygen > 3 mg/L) were determined using dynamic light scattering (DLS) with a Zetasizer Nano ZS (Malvern Instruments). The nominal concentrations were set as 0.1 mg/L, 1 mg/L, and 10 mg/L, respectively.

2.3. Culturing of D. magna

D. magna was cultured in an artificial climate incubator (MGC350HP-2, Hengyi, China) and fed daily with *Chlorella pyrenoidosa* (1×10^6 cells/mL). The culture solution was prepared from dechlorinated tap water, which was aerated for three days and saturated with dissolved oxygen. The incubator temperature was maintained at 20 ± 1 °C, and the light/dark cycle ratio was set at 16:8. Neonates <24 h were selected as test organisms in this study. All exposure experiments were carried out in the test water.

2.4. Exposure experiment

2.4.1. Acute toxicity

The acute immobilization tests on *D. magna* were performed according to OECD guideline 202(OECD 2004). A stock suspension of BPNS was gradually diluted using standard dilution water to obtain suspensions of BPNS with the following concentrations: 0.1, 1, 2.2, 4.8, 10, 25 and 50 mg/L. Three replicates were tested for each treatment and each test vessel contained 50 mL of test medium and five *D. magna* neonates (6~24 h). Immobilisation (*I*, %) was employed as the endpoint of mortality assessment, and was defined as the lack of movement for 15 s after gentle shaking of the test vehicle. At the end of the exposure, surviving *D. magna* was transferred to a clean slide and the distribution of BPNS in *D. magna* was observed using a light microscope (BK6000).

2.4.2. Growth and reproduction assay

Survival rate, body length, behavioral changes, and hatching success were monitored. Reproductive impairment, quantified by neonate production and time-to-first brood, and developmental abnormalities, such as molting frequency and thoracic limb beat frequency, were assessed in compliance with OECD guideline 211. Test concentrations were established based on the EC_{10} values obtained from acute toxicity data. *D. magna* was exposed to BPNS exposure solutions of 0.01, 0.03, 0.09, 0.28 and 0.81 mg/L for 21 d, with ten parallel groups were set up for each treatment. The test medium was renewed every two days. During the test period, the time of first laying, number of litters, number of litters per laying, and number of shedding were recorded for each *D. magna*. Exposed *D. magna* bodies were placed on slides and imaged with a light microscope (BK6000, Chongqing Aote Optical Instrument Co., Ltd.), and *D. magna* body lengths were measured with CAM-MS software (v2.1.3.250, CHN). *D. magna* body heart rate and thoracic limb beating frequency were measured with a microscope and a stopwatch.

2.5. Oxidative stress test

2.5.1. Detection of ROS in D. magna

2′,7′-dichlorodihydrofluorescein diacetate (DCFH-DA) was used to detect ROS production. This probe can pass through the cell membrane, and the intracellular ROS can oxidize non-fluorescent 2′,7′-dichlorodihydrofluorescein (DCFH) to produce fluorescent 2′,7′-dichlorofluorescein (DCF)(Wang et al., 2020). After 24 and 48 h of exposure, five *D. magna* individuals in each group were selected, washed three times using standard dilution water, and then transferred to 10 μM DCFH-DA. After 30 min of dark incubation, the sampled *D. magna* were transferred to centrifuge tubes containing normal saline (0.85 %) and immediately homogenized using a nucleic acid isolation machine (MP Fastprep24 5 G, USA). The operating conditions were: speed - 5 m/s, time - 40 s. The fluorescence intensity (E_x/Em = 488/525 nm) of the control group and the test group was measured using a microplate reader (VL0000D1, Thermo Fisher Scientific, USA). The relative content of ROS is expressed as %, as shown by the following formula:

$$\text{Total ROS relative content \%} = \left(\frac{\text{test group average fluorescence intensity}}{\text{control group average fluorescence intensity}}\right) \times 100\%$$

Under the same conditions, the ROS in the treated *D. magna* were visualized using fluorescence microscopy (Ts2R-FL, Nikon Corporation, Japan).

2.5.2. Biochemical marker assay

D. magna exposed to BPNS (0, 0.1, and 1.0 mg/L) were sampled after 24 h or 48 h of exposure. Groups of 30 *D magna* were collected independently and washed three times using standard dilution water, and the polyhydric liquid on the surface of *D. magna* was dried. According to the ratio of weight (g): volume (mL) = 1:9, a moderate volume of a phosphate buffer solution (PBS) was added in a lysing matrix dialysis tube containing the treated *D. magna*. All samples were collected by centrifugation at 3500 rpm/min for 10 min at 4 °C. The enzyme activities of catalase (CAT), superoxide dismutase (SOD) and the malondialdehyde (MDA) content in *D. magna* were measured using their respective assay kits (Nkoom et al., 2019a, 2019b).

2.6. RNA sequencing

A BPNS dispersion was diluted step by step into 0.01, 0.09 mg/L BPNS exposure suspension, and BPNS was evenly dispersed by ultrasonic treatment before exposure. Each beaker was filled with 50 *D magna* larvae and 1 L BPNS exposure solution. The test medium was refreshed every two days, and the whole experiment lasted 21 d. After exposure, each sample was rapidly cryogenically frozen using liquid nitrogen. After rapid freezing, the sample was stored in a −80 °C refrigerator. Subsequently, the mRNA of *D. magna* samples was sequenced using Illumina's second-generation high-throughput sequencing platform (Ovisen Genentology Co., Ltd.).

2.7. Bioinformatics analysis

Reads containing a small amount of joint pollution and low quality pollution were filtered, and the distribution of Q_{20}, Q_{30} and base contents of filtered Reads were calculated to evaluate the data quality. Based on the reference genome and annotation file of *D. magna* (https://www.ncbi.nlm.nih.gov/genome/?term=Daphnia+magna), the STAR software was selected to perform alignment analysis on high quality Reads. the gene expression abundance was quantified using the normalized FPKM (Fragments per kilobase of exon model per million mapped reads)(Mortazavi et al., 2008). Gene Ontology (GO, http://www.geneontology.org/) enrichment analysis of DEGs was implemented by the GOseq R package. GOseq software(Young et al., 2010) was used for GO enrichment analysis. GO terms with corrected P-value < 0.01 were considered significantly enriched by differential expressed genes. Systematic analysis of differences in metabolic pathway using Kyoto Encyclopedia of Genes and Genomes (KEGG, http://www.kegg.jp)(Kanehisa et al., 2008). The significantly enriched KEGG pathways were identified by corrected P-value < 0.05.

2.8. Statistical analysis

All statistical analyses were conducted with Origin 2018 (Origin Lab, USA) and SPSS Statistics 26 (IBM, USA). The data are presented as the mean ± standard error of the mean. To distinguish significant differences between the control and treatment groups, one-way analysis of variance was performed and post hoc multiple comparison (Duncan's test) was executed using SPSS 26.0 software. A statistically significant difference between the control and treatment groups was indicated by $p < 0.05$.

3. Results and discussion

3.1. Characterization of the BPNS

As depicted in Fig. 1A, the exfoliated BPNS excellent dispersion in ultrapure water. The BPNS displayed irregular lamellar structures with smooth surfaces as observed in the TEM and SEM images (Fig. 1B and 1C). Atomic force microscopy (AFM) analysis of 125 BPNS datasets revealed an average lateral size and thickness of 73 ± 59 nm and an average thickness 1.8 ± 0.8 nm (Fig. 1D and 1E). The zeta potential of BPNS was measured to be −29.6 ± 0.4 mV, with an average hydrodynamic diameter of 337 ± 88 nm (Fig. 1F and 1G). Wu et al. (2020) used DLS to determine the zeta point and hydrodynamic diameter of BP in the range of −3.5∼ −16.4 mv and 448.8 ∼1500.6 nm, respectively. It is important to note that the hydrodynamic diameter measured by DLS does not represent the absolute particle size due to the nonspherical morphology of BPNS (Zhou et al., 2021). Therefore, the DLS measured diameter was primarily used to assess changes in particle size rather than absolute dimensions.

The stability of nanomaterials is a critical factor influencing their toxicological effects. To evaluate this, the particle size and zeta potential of BPNS suspensions were monitored over time (Table S1). During the exposure period, the average hydrodynamic diameter of BPNS initially decreased and subsequently increased. After 48 h of exposure, the average hydrodynamic diameter of the BPNS at concentrations of 0.1, 1 and 10 mg/L increased by 11.9 %, 33.0 %, and 31.8 %, respectively. These findings suggest that BPNS tend to aggregate and settle over time. The zeta potential of the BPNS ranged from −13.6 ± 0.9 mV to −19.6 ± 0.3 mV. In contrast, a zeta potential of approximately −43.4 mV is generally considered indicative of a stable BP nanofluid system (Fekete-Kertesz et al., 2020). The experimentally observed zeta potential values indicat that the BPNS in the *D. magna* medium were in an unstable state, predisposing them to aggregation and sedimentation.

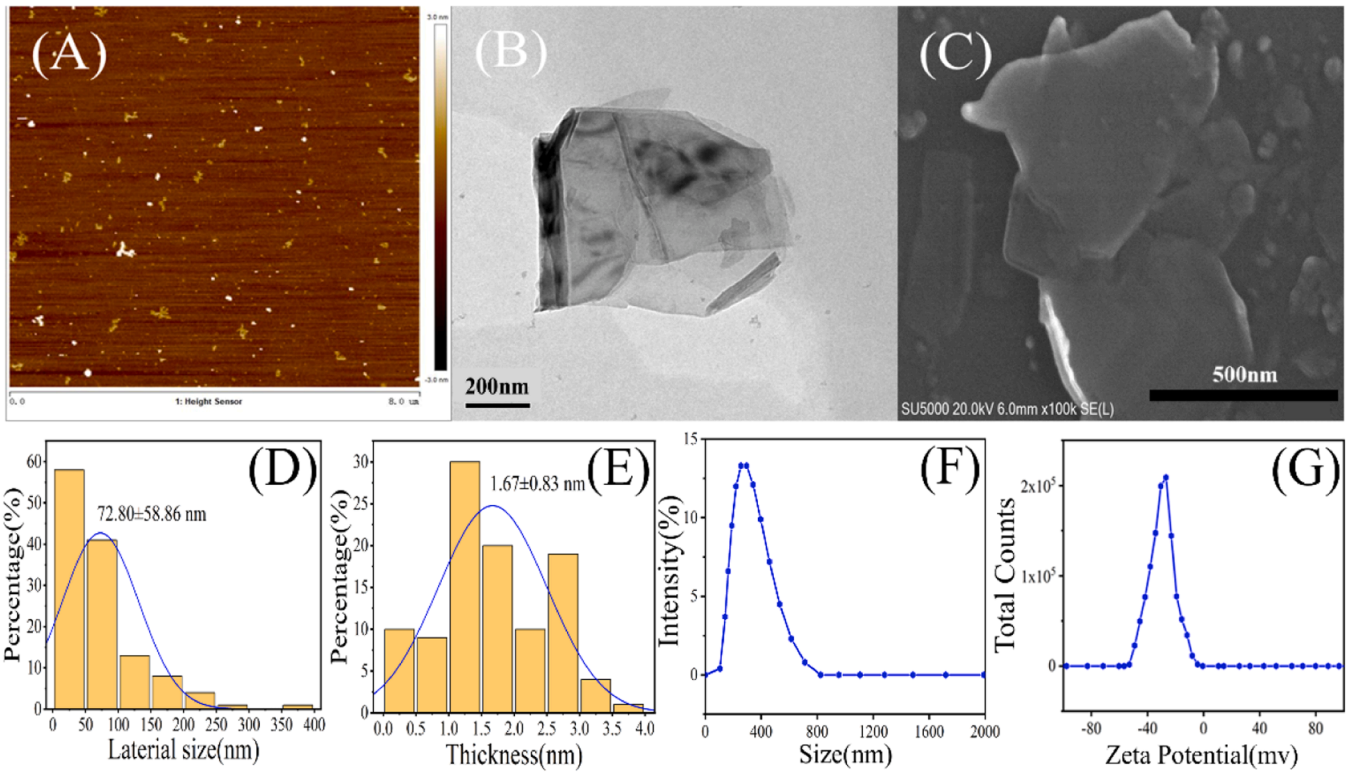

Fig. 1. Characterization of BPNS. (A) AFM, (B) TEM, and (C) SEM image of BPNS; Statistical analysis of the (D) lateral size and (E) thickness of BPNS by AFM measurements; (F) hydrodynamic size distribution, and (G) Zeta potential distribution. The scale bars in (B) and (C) represent 200 and 500 nm, respectively. The distributions are derived from quantitative measurements performed on multiple AFM images acquired at different regions of the same sample under identical magnification.

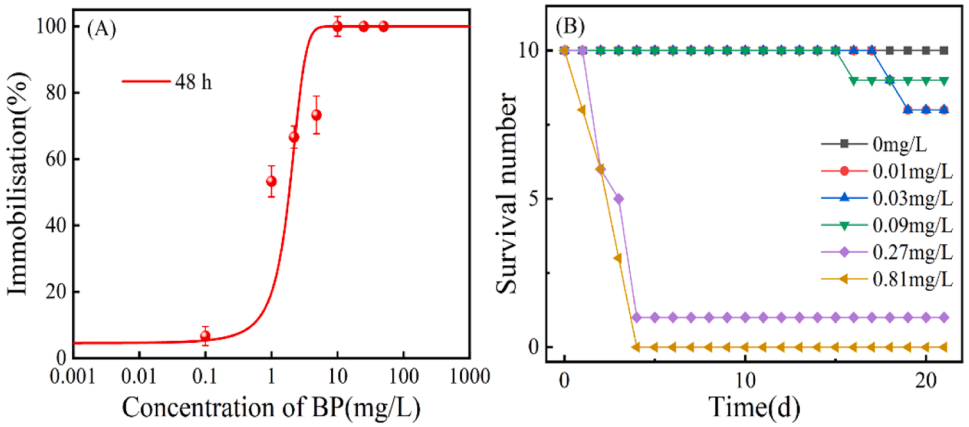

Fig. 2. Inhibitory effects of BPNS on *D. magna* were evaluated under two distinct exposure regimes: (A) acute exposure and (B) chronic exposure.

3.2. Toxicity of BPNS to D. magna

The acute toxicity of BPNS to *D. magna* has not been previously documented. In this study, no significant behavioral inhibition was observed in *D. magna* during the initial 24 h exposure period at BPNS concentrations below 10 mg/L. However, under prolonged exposure (36-48 h), pronounced inhibitory effects were observed except at the lowest concentrations (0.1 mg/L and 1.0 mg/L). These findings indicate that the toxic effects of BPNS on *D. magna* are both time- and concentration-dependent (Fig. 2A). Notably, substantial black particulate matter was detected in the intestinal tracts of (Fig. S1), suggesting that BPNS appeared to migrate through the intestinal coils (Text S2). The 48 h EC_{50} for *D. magna* immobilization by BPNS was calculated to be 1.9 mg/L (Table S2). According to the Organization for Economic Cooperation and Development classification criteria, BPNS exhibited acute toxicity to *D. magna*, categorized as acute grade II.

The chronic toxicity of BPNS to *D. magna* was also investigated, as shown in Fig. 2B. During the first four days of exposure, BPNS at 0.27 mg/L significantly inhibited *D. magna* activity, while 0.81 mg/L BPNS resulted in complete inhibition. After 21 d of exposure, inhibition rates of 20 %, 10 %, 90 %, and 100 % were observed at BPNS concentrations of 0.03, 0.09, 0.27, and 0.81 mg/L, respectively. These results further underscore the time and concentration-dependent nature of BPNS toxicity in chronic exposure scenarios.

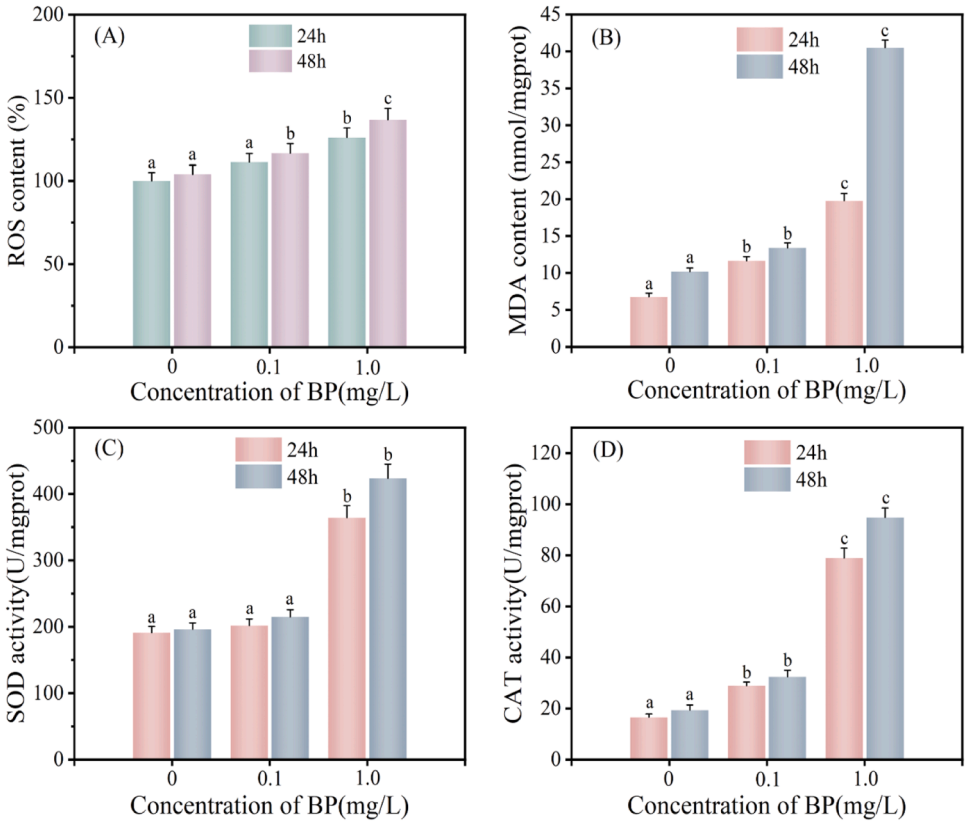

Fig. 3. (A) Concentration and duration dependent alterations in the relative levels of reactive oxygen species (ROS) in *D. magna* following BPNS exposure. (B–D) impacts of BPNS on oxidative stress biomarkers: (B) MDA content, (C) SOD activity, and (D) CAT activity in *D. magna*.

3.3. Oxidative stress test

3.3.1. Effects of BPNS on ROS formation in D. magna

The relative content of ROS in *D. magna* increased with the exposure concentration and exposure time of BPNS (Fig. 3A). Compared with the control group, the relative ROS content in *D. magna* exposed to BPNS at 0.1 mg/L and 1.0 mg/L after 24 h exposure was 108.2 and 123.4 %, respectively. After 48 h of exposure, the relative content of ROS in *D. magna* exposed to BPNS at 0.1 mg/L and 1.0 mg/L was increased to 111.5 and 128.5 %, respectively. The higher concentration of BPNS (1.0 mg/L) thus significantly induces more ROS generation in *D. magna* compared with the control group. These results suggest that exposure to BPNS can induce ROS accumulation in *D. magna* and then leads to oxidative stress. In addition, this result is further corroborated by the presence of significant ROS fluorescence signals in *D. magna* exposed to high concentrations of BPNS (Text S3, Fig. S2).

3.3.2. Effect of BPNS on enzyme activity of D. magna

The changes of MDA content in *D. magna* exposed to BPNS are shown in Fig. 3B. BPNS at 0.1 or 1.0 mg/L increased the MDA contents in *D. magna* as compared with the control group after 24 h of exposure. Moreover, the lengthening of the exposure time significantly increased the MDA contents in *D. magna* exposed to 1.0 mg/L of BPNS. Some studies have shown that ROS produced in the body can react with polyunsaturated fatty acids in biofilms, causing lipid peroxidation and thus forming lipid peroxides. Lipid peroxide MDA is often used as one of the markers to reflect the degree of biofilm damage(Wang et al., 2025). The content of MDA thus often reflects the degree of lipid peroxidation in the body(Lee et al., 2024; Yuan and Zhang, 2025). The results of our study showed that exposure to BPNS resulted in excessive ROS formation, enhanced lipid peroxidation, and damaged cell membranes.

SOD and CAT are the main antioxidant enzymes that can scavenge extra ROS and promote healthy cells in the physique. SOD is the first line of defense in the antioxidant system. It can target oxygen radicals and catalyze the conversion of $O_2^{-}\cdot$ to H_2O_2. H_2O_2 is still a substance with oxidant toxicity in *vivo*. CAT can degrade H_2O_2 to water and oxygen (Li and Ko, 2012; Li et al., 2021). Elevated SOD activity in *D. magna* after exposure to 0.1 and 1.0 mg/L BPNS (Fig. 3C) is induced because excessive ROS may have increased SOD activity to defend the *D. magna* against oxidative stress. After 48 h of exposure, the CAT activity in *D. magna* increased by 67.6 and 391 %, respectively compared to the control group (Fig. 3D). Judging from the increase in CAT, prolonged exposure to BPNS causes oxidative damage to organisms, forcing organisms to increase CAT activity to remove excess H_2O_2. From the results it can be inferred that the production of free radicals increases in *D. magna* under chemical stress. Thus, excessive ROS may have increased the activity of SOD and CAT to defend itself against oxidative stress.

3.4. Growth and reproduction responses

Exposure to low concentrations of 0.01, 0.03, and 0.09 mg/L of BPNS resulted in earlier time to first parturition and an increased number of births in *D. magna* compared to controls. The high exposure concentration (0.27 mg/L) showed no significant differences in response compared to the control group. Similarly, the first litter number and average litter number of exposed *D. magna* showed the same trend (Fig. 4A and 4B). Studies have shown that in an aquatic water environment with low pollution levels, *D. magna* can maintain the normal reproduction capacity of its population by adjusting the time of sexual maturity and the number of single offspring. That is to compensate for the environmental stress caused by environmental stress(An et al., 2022). Therefore, the above results suggest that *D. magna*, living for a long time in a water environment containing low concentrations of

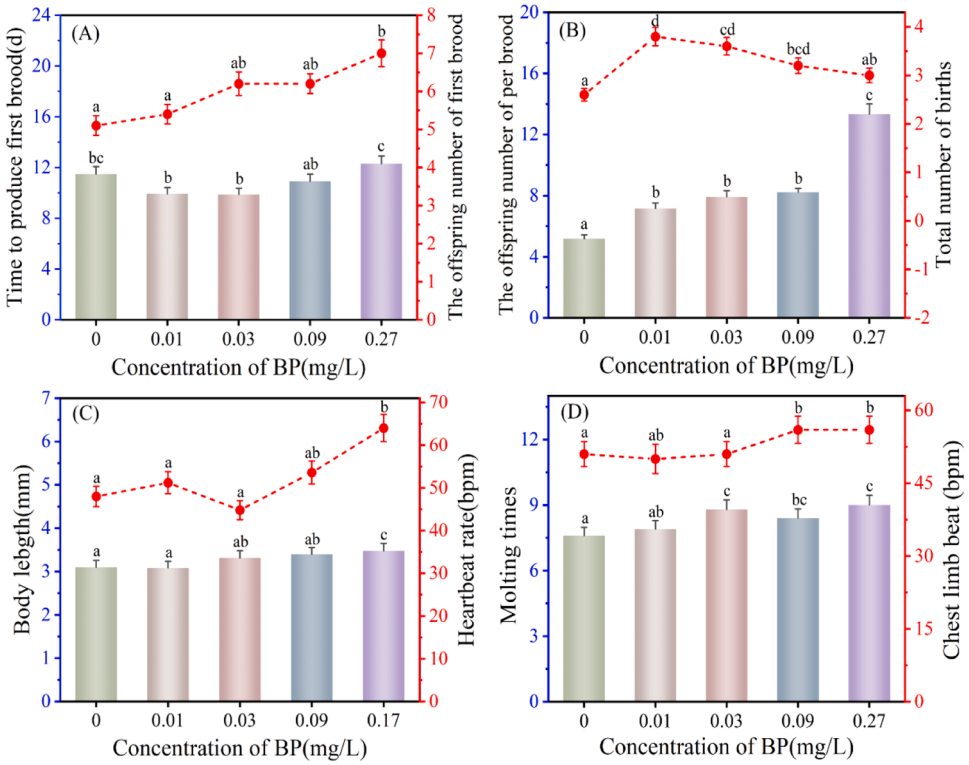

Fig. 4. Reproductive and developmental toxicity of BPNS in *D. magna*: (A) time and number of first births; (B) average number and total number of births; (C) body length and heartbeat rate; (D) thoracic limb movement frequency and number of molts.

BPNS, responds to the damage caused by BPNS through reproductive changes.

Contrary to reproductive outcomes, the body length, heart rate and thorax beat frequency of *D. magna* did not change significantly at low concentrations of 0.01, 0.03 and 0.09 mg/LBPNS, but increased significantly at high concentrations of 0.27mg/L (Fig. 4C and 4D). Compared with the control group, the times of molt of *D. magna* increased under different concentrations of BPNS. Physiological indexes such as body length, heart rate, chest and leg beating frequency can reflect the changes of growth and development, feeding behavior and of the blood circulatory system of *D. magna* under the influence of pollutants(Huang et al., 2011; Pan et al., 2017; Tkaczyk et al., 2021). The results showed that the increase of the heart rate and the beating frequency of the chest and limb may be due to the intake of more energy in response to the damage caused by BPNS, and with the increase of energy intake, the basic metabolism of *D. magna* was improved.

3.5. Analysis of differentially expressed genes (DEGs) and GO enrichment

Transcriptional analyses of *D. magna* were performed to further understand the molecular mechanisms behind BPNS-induced chronic toxicity. More DEGs were found in the 0.01 mg/L exposure group than in the 0.09 mg/L exposure group, with a total of 1818 DEGs. Compared with the control treatment, there was more up-regulation than down-regulation of differential genes in *D. magna* under BPNS exposure, indicating that BPNS altered the differential gene expression of *D. magna* to different degrees. Cluster plot analysis showed that BPNS altered the gene expression pattern of *D. magna* (Fig. 5A-5D).

The enriched GO terms are shown in Fig. 5E and 5F. Metal ions play important roles in maintaining normal physiological processes in organisms, such as ATP, DNA and protein synthesis. Compared with controls, enriched genes were mainly associated with ion homeostasis, including cellular transition metal ion homeostasis and iron ion homeostasis. It has been shown that iron homeostasis in organisms is associated with oxidative stress. In the present study, structural components of the stratum corneum and chitin-binding processes were significantly enriched. The Genes involved in cuticle formation are essential for molting in *D. magna*, and chitin contributes to chitin bioactivities such as antibacterial, immune stimulation and promotion of wound healing. The significant up-regulation of these genes suggests that detoxification is a common feature of the response to stress in *D. magna*. In studies elucidating the toxicity mechanisms of graphene in *D. magna*, analogous upregulation of stress-responsive genes was observed, further indicating that *D. magna* activates self-regulatory pathways to counteract environmental stressors(Huang et al., 2023).

Furthermore, differential expression of genes for carbohydrate metabolic processes and glycosyl hydrolase activity was significantly enriched to provide more energy for detoxification compared to controls. Similarly, differentially expressed genes for serine proteases, a type of endopeptidase found to be involved in digestion, development and immunity, were significantly enriched in *D. magna* compared to controls. When *D. magna* was subjected to a variety of stress responses brought about by external stimuli, a number of peptidases, including serine protease, were significantly enriched in the body. These results indicated that *D. magna* accelerates the detoxification process of BPNS by increasing the expression of relevant differential genes.

3.6. KEGG pathway analysis of DEGs

KEGG enrichment analysis demonstrated the top 20 pathways exhibiting the most significant differential gene enrichment in both groups, predominantly within the primary pathways of metabolism, cellular processes, and environmental information processing. Notably, higher numbers of differentially expressed genes were observed in the pathways of ascorbate and aldarate metabolism, starch and sucrose metabolism, and steroids. The differentially expressed genes in these enriched pathways were predominantly up-regulated genes compared to the controls (Fig. 6).

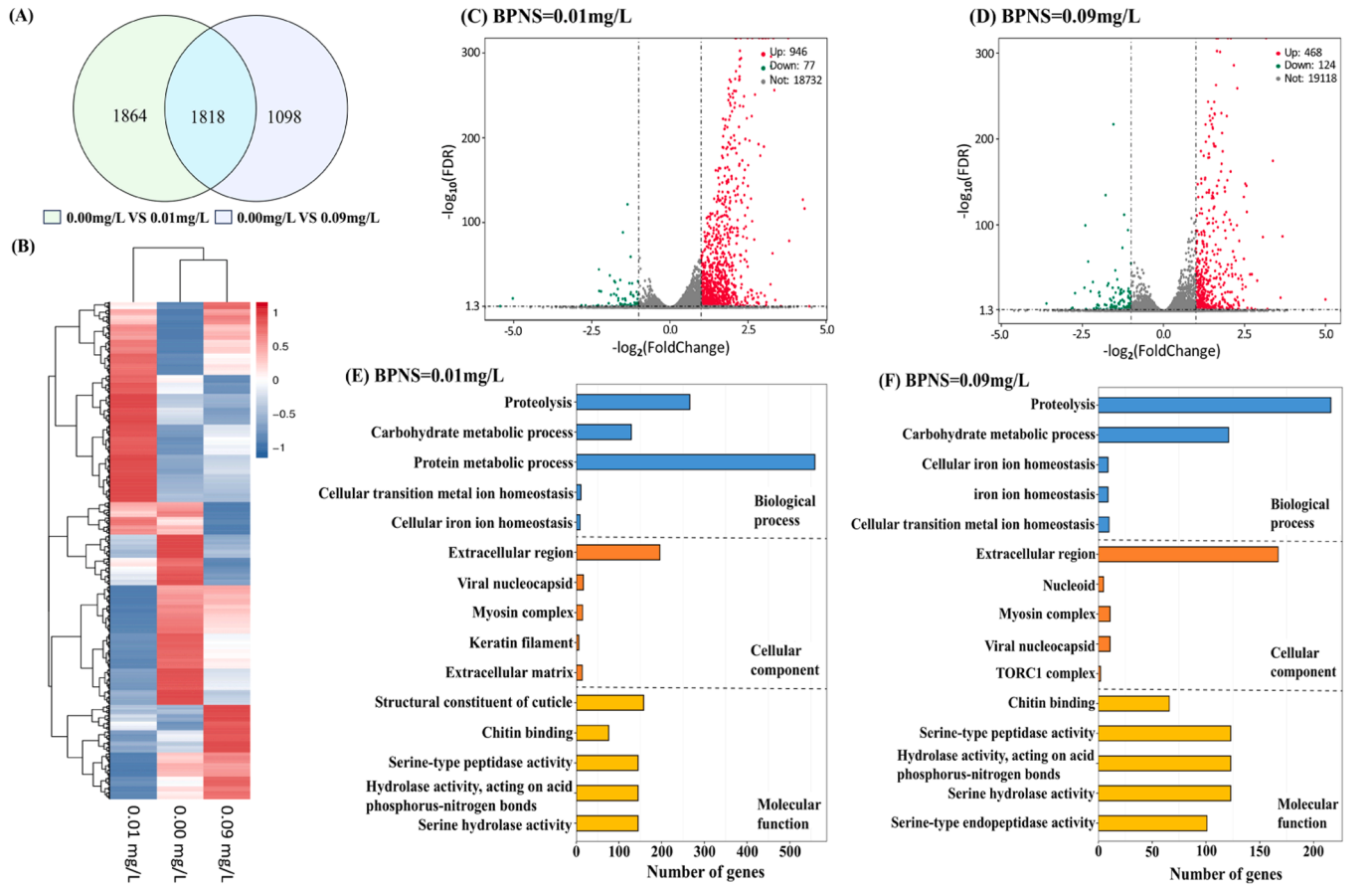

Fig. 5. Transcriptomic profiling of BPNS-exposed *D. magna*: (A) venn diagram of DEGs in the exposure groups; (B) hierarchical clustering of DEG expression profiles; (C, D) dose-responsive differential expression (volcano plots) at 0.01 and 0.09 mg/L BPNS, respectively; (E, F) the five most significantly enriched GO pathways in the samples collected from the 0.01 and 0.09 mg/L groups. The value of the horizontal axis represents strength.

Exposure to BPNS induced significant upregulation of lysosomal pathway-associated genes in cellular processes and signaling, including those encoding acid hydrolases (e.g., *gba*) and membrane proteins (e.g., *lamp*). As central degradation hubs, lysosomes counteract BPNS-mediated metabolic perturbations through coordinated mechanisms: the increased expression of glucocerebrosidase (*gba*) enhances lipid catabolism to alleviate BPNS-induced glycolipid accumulation in *D. magna*, while elevated acid ceramidase (*asah*1) levels suggest a dynamic equilibrium between ceramide-activated pro-apoptotic pathways (e.g., p53 signaling) and antioxidant defenses. Furthermore, studies have demonstrated that BPNS and graphene, owing to their sharp-edged layered structures, exhibit a "nano-knives effect", causing physical damage to bacterial cell membranes (Xiong et al., 2018; Chaloupsky et al., 2024; Pham et al., 2015). Concurrently, the overexpression of lysosomal membrane proteins (*lamp*) likely mitigates such "nano-knives effect" membrane injury by reinforcing lysosomal integrity to prevent enzymatic leakage. These findings collectively underscore an adaptive cellular strategy to counteract both biochemical and physical disruptions caused by BPNS, highlighting the critical role of lysosomal pathway activation in maintaining cellular homeostasis under nanomaterial stress.

Genes associated with the enzymatic antioxidant system, purine metabolism and retinol metabolism were significantly up-regulated in the antioxidant system signaling passages. The increase of ROS in vivo under BPNS exposure in *D. magna* stimulates the antioxidant defense system, leading to oxidative stress. Up-regulation of genes in the enzymatic and non-enzymatic antioxidant systems can mitigate the damage coming from oxidative stress (Wang et al., 2021). The upregulation of *sod* and *cat* in the enzymatic antioxidant system aligns with their roles in ROS scavenging: SOD converts $O_2^{-}\cdot$ to H_2O_2, which is subsequently neutralized by *cat* into H_2O and O_2, leading to a significant reduction in ROS levels(Calvani et al., 2022; Sun et al., 2012). In the non-enzymatic system, xanthine dehydrogenase gene (*xdh*)driven uric acid synthesis effectively quenches ·OH radicals, while *dhrs4* enhances vitamin A bioavailability by modulating retinol metabolism(Malea et al., 2022), thereby amplifying its antioxidant capacity to counteract oxidative stress.

The major pathways significantly enriched in metabolic signaling pathways are glucose metabolism, lipid metabolism and amino acid metabolism. During glucose metabolism, up-regulation of related genes can catalyze enzymatic reactions to generate more ascorbic acid (AsA). In the ascorbic acid pathway, EC 1.13.99.1 is a redox-related enzyme that catalyzes the reduction of nitrite (NO_2^-) to nitric oxide (NO). NO contributes to antioxidant defense by activating antioxidant genes (e.g., SOD) or directly scavenging ROS, thereby establishing a secondary antioxidant barrier. AsA alleviates BPNS-induced oxidative stress through direct ROS neutralization and regeneration of other antioxidants (e.g., vitamin E). The upregulation of EC 1.13.99.1 may indirectly support this process by modulating NO levels. Furthermore, AsA mitigates oxidative damage caused by BPNS by chelating free iron ions(Pal and Jana, 2020; Wang et al., 2022), thereby suppressing Fenton reaction-driven ROS generation ($Fe^{2+} + H_2O_2 \rightarrow$ ROS).

Furthermore, genes for starch and sucrose metabolism and galactose metabolism were significantly up-regulated. This is consistent with the gene expression of glycosyl compound hydrolases in GO enrichment, all providing energy for large stilbene detoxification. In the lipid metabolism pathway, BPNS affects the biosynthesis of steroids, including sterols and steroid hormones. EC 1.3.1.72 is a key enzyme involved in

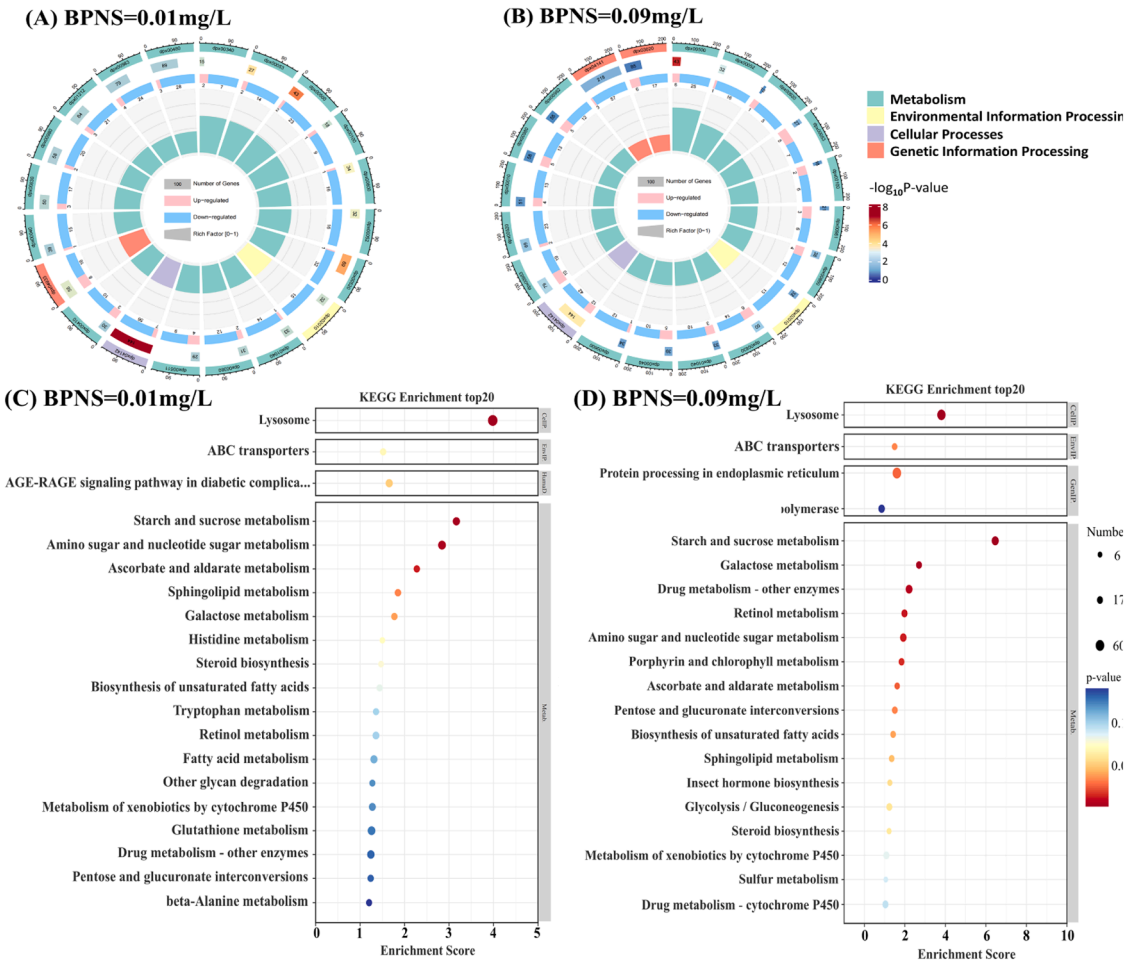

Fig. 6. Signaling pathway analysis of *D. magna* exposed to BPNS. Top 20 enriched KEGG pathways induced by 0.01 mg/L and 0.09 mg/L BPNS. Bubble size corresponds to the number of DEGs per pathway; color intensity reflects the enrichment significance (-$\log_{10}$(*P* value)).

steroid biosynthesis. In arthropods such as insects, its homologous enzyme participates in the process of synthesizing ecdysone from cholesterol precursors. For *D. magna*, the upregulation of EC 1.3.1.72 may accelerate the steps of steroid synthesis, leading to an increase in the synthesis amount of ecdysone and other related steroid hormones. Ecdysone plays a central role in the growth and development of *D. magna*, promoting molting. If the synthesis of ecdysone increases abnormally, it will change the molting frequency of *D. magna*, interfere with the normal growth rhythm, affect the body size and development rate, and thus indirectly have an adverse effect on the reproductive ability. In amino acid signaling metabolism, BPNS significantly affected histidine biosynthesis compared to controls. This may be attributed to the accumulation of BPNS in the gut, which caused damage to the gastrointestinal mucosa of the *D. magna*, whereas histidine could alleviate the damage caused by inflammation. These results suggest that BPNS significantly interfered with the physiological processes of glucose metabolism, lipid metabolism and amino acid metabolism in the metabolic pathway.

3.7. RNA quality control

Sequences and base contents after quality control were >95 % of those before quality control, Q_{20} was >97.9 %, and Q_{30} was >93.9 % (Table S3). The ratio of Total Mapped Reads or Fragments that can be compared to reference sequences is higher than 96 %. (Table S4). Correlation examination and PCA analysis were performed on the transcriptomes among all samples, and it was found that R^2 values in correlation examination were ≥0.971 (Fig. S3), indicating a high correlation among all samples. In summary, the RNA sequencing results of all samples in this study were reliable.

4. Conclusions

Suspensions of BPNS are unstable in aquatic environments and tend to aggregate and deposit. The 48h-EC_{50} of *D. magna* exposed to BPNS was 1.9 mg/L, which entitles the BPNS as being Level II toxic according to OECD standards. BPNS not only accumulated in the intestinal tract of *D. magna*, but also showed yellow and red 'fat bubbles' around the intestine, which indicated that high concentrations of BPNS could affect lipid metabolism in *D. magna*. After chronic exposure (21 d), BPNS reduced the survival rate of *D. magna*, inhibited its growth and reproduction, and affected its reproduction and development. This demonstrated that BPNS poses a hazard risk to the aquatic environment. Further transcript sequencing showed that, compared with the control group, most of the differential genes were enriched in molecular functions, and the expression of the differential genes in these processes promoted the detoxification reaction by *D. magna* of BPNS. The regulation of energy and cuticle pathways may be the main reasons for the increase of the heart rate, the beating frequency of the chest limbs and the number of molting of *D. magna*. The regulation of the pathway of KEGG concentration and significant enrichment may be an effective means for *D. magna* to deal with the oxidative stress reaction and the " nano-knife effect " injury caused by BPNS. In the lipid metabolism signaling pathway, *D. magna* may up-regulate the genes in the steroid

pathway, advance the sexual maturity time, increase litter size and litter frequency, and thus compensate for BPNS stress.

CRediT authorship contribution statement

Tianlie Luo: Writing – review & editing, Funding acquisition. **Ping Zhang:** Writing – original draft, Data curation. **Jinyu Wang:** Visualization, Conceptualization. **Jingjing Shi:** Writing – review & editing, Visualization. **Yubo Di:** Data curation, Conceptualization. **Guo Liu:** Writing – review & editing, Resources, Conceptualization. **Willie J.G.M. Peijnenburg:** Visualization, Resources, Writing – review & editing.

Declaration of competing interest

The authors declare that they have no known competing financial interests or personal relationships that could have appeared to influence the work reported in this paper.

Acknowledgements

This study was supported by National Natural Science Foundation of China (42307375), the State Environmental Protection Key Laboratory of Synergetic Control and Joint Remediation for Soil & Water Pollution Open Fund (GHBK-2020-011), and the Scientific Research Foundation of CDUT (10912-KYQD2019-07746).

Supplementary materials

Supplementary material associated with this article can be found, in the online version, at doi:10.1016/j.aquatox.2025.107333.

Data availability

Data will be made available on request.

References

An, X., Lui, X., Jiang, J., Wang, F., Lv, L., Li, G., Wu, S., Zhao, X., 2022. Acute and chronic toxicities of prothioconazole and its metabolite prothioconazole-desthio in *Daphnia magna*. Environ. Sci. Pollut. Res. 29, 54467–54475. https://doi.org/10.1007/s11356-021-17863-y.

Bigham, A., Serrano-Ruiz, M., Caporali, M., Fasolino, I., Peruzzini, M., Ambrosio, L., Raucci, M.G., 2024. Black phosphorus-based nanoplatforms for cancer therapy: chemistry, design, biological and therapeutic behaviors. Chem. Soc. Rev. https://doi.org/10.1039/d4cs00007b.

Calvani, N.E.D., Verissimo, C.D.M., Jewhurst, H.L., Cwiklinski, K., Flaus, A., Dalton, J.P., 2022. Two distinct superoxidase dismutases (SOD) secreted by the Helminth Parasite *Fasciola hepatica* play roles in defence against metabolic and host immune cell-derived reactive oxygen species (ROS) during growth and development. Antioxidants 11. https://doi.org/10.3390/antiox11101968.

Cao, X., Chen, L., Fan, Y., Fu, M., Du, Q., Chang, Z., 2024. Black phosphorus quantum dots induced neurotoxicity, intestinal microbiome and metabolome dysbiosis in zebrafish (Danio rerio). Sci. Total. Environ. 954. https://doi.org/10.1016/j.scitotenv.2024.176644, 176644-176644.

Chaloupsky, P., Kolackova, M., Dobesova, M., Pencik, O., Tarbajova, V., Capal, P., Svec, P., Ridoskova, A., Bytesnikova, Z., Pelcova, P., Adam, V., Huska, D., 2024. Mechanistic transcriptome comprehension of Chlamydomonas reinhardtii subjected to black phosphorus. Ecotoxicol. Environ. Saf. 270. https://doi.org/10.1016/j.ecoenv.2023.115823.

Chen, C., Guo, L., Shen, Y., Hu, J., Gu, J., Ji, G., 2024. Oxidative damage and cardiotoxicity induced by 2-aminobenzothiazole in zebrafish (*Danio rerio*). J. Hazard. Mater. 476. https://doi.org/10.1016/j.jhazmat.2024.135032.

Deng, S., Zhao, Q., Liu, D., Xiong, Z., Zhang, S., Zhang, X., Wu, F., Xing, B., 2024. Black phosphorus nanosheets induce autophagy dysfunction by a size- and surface modification-related impairment of lysosomes in macrophages. Ecotoxicol. Environ. Saf. 285. https://doi.org/10.1016/j.ecoenv.2024.117073.

Fekete-Kertesz, I., Laszlo, K., Terebesi, C., Gyarmati, B.S., Farah, S., Marton, R., Molnar, M., 2020. Ecotoxicity assessment of graphene oxide by *Daphnia magna* through a multimarker approach from the molecular to the physiological level including behavioral changes. Nanomaterials 10. https://doi.org/10.3390/nano10102048.

Gu, J., Lin, D., Sun, Y., Guo, Y., Chen, B., Zhang, Y., Liu, F., 2022. Integrating transcriptome and physiological analysis to reveal the essential responses of *Daphnia magna* to antimony trioxide nanoparticle. J. Hazard. Mater. 437. https://doi.org/10.1016/j.jhazmat.2022.129303.

He, C., Ruan, F., Jiang, S., Zeng, J., Yin, H., Liu, R., Zhang, Y., Huang, L., Wang, C., Ma, S., Zuo, Z., 2020. Black phosphorus quantum dots cause nephrotoxicity in organoids, mice, and Human cells. Small. 16. https://doi.org/10.1002/smll.202001371.

Huang, Q., Fang, C., Wu, X., Fan, J., Dong, S., 2011. Perfluorooctane sulfonate impairs the cardiac development of a marine medaka (*Oryzias melastigma*). Aquat. Toxicol. 105, 71–77. https://doi.org/10.1016/j.aquatox.2011.05.012.

Huang, Y., Yao, H., Li, X., Li, F., Wang, X., Fu, Z., Li, N., Chen, J., 2023. Differences of functionalized graphene materials on inducing chronic aquatic toxicity through the regulation of DNA damage, metabolism and oxidative stress in *Daphnia magna*. Sci. Tot. Environ. 876. https://doi.org/10.1016/j.scitotenv.2023.162735.

Kanehisa, M., Araki, M., Goto, S., Hattori, M., Hirakawa, M., Itoh, M., Katayama, T., Kawashima, S., Okuda, S., Tokimatsu, T., Yamanishi, Y., 2008. KEGG for linking genomes to life and the environment. Nucleic. Acids. Res. 36, D480–D484. https://doi.org/10.1093/nar/gkm882.

Lee, Y., Kim, D.-H., Lee, J.-S., Kim, H.S., Maszczyk, P., Wang, M., Yang, Z., Wang, D.-Z., Lee, J.-S., 2024. Combined exposure to hypoxia and nanoplastics leads to negative synergistic oxidative stress-mediated effects in the water flea *Daphnia magna*. Mar. Pollut. Bull. 202. https://doi.org/10.1016/j.marpolbul.2024.116306.

Li, J.H., Ko, Y.C., 2012. Plasticizer incident and its health effects in Taiwan. Kaohsiung. J. Med. Sci. 28, S17–S21. https://doi.org/10.1016/j.kjms.2012.05.005.

Li, N., Xu, Z., Yao, H., Chen, J., Li, X., 2021. Impact of particle size of zinc oxide nanoparticles on its bioaccumulation and oxidative stress responses. Chinese Sci. Bull. 66, 3219–3226. https://doi.org/10.1360/TB-2021-0186.

Li, P., Zeng, L., Gao, J., Yao, L., Zhao, X., Wu, Q., Liu, X., Wang, Y., Yang, X., Shi, J., Hu, L., Qu, G., Cai, Z., Jiang, G., 2020. Perturbation of normal algal growth by black phosphorus nanosheets: the role of degradation. Environ. Sci. Technol. Lett. 7, 35–41. https://doi.org/10.1021/acs.estlett.9b00726.

Lu, Y., Zhang, H., Wang, H., Ma, N., Sun, T., Cui, B., 2021. Humic acid mediated toxicity of faceted TiO_2 nanocrystals to *Daphnia magna*. J. Hazard. Mater. 416. https://doi.org/10.1016/j.jhazmat.2021.126112.

Malea, P., Kokkinidi, D., Kevrekidou, A., Adamakis, I.-D.S., 2022. The enzymatic and non-enzymatic antioxidant system response of the Seagrass *cymodocea nodosa* to bisphenol-A toxicity. Int. J. Mol. Sci. 23. https://doi.org/10.3390/ijms23031348.

Mortazavi, A., Williams, B.A., McCue, K., Schaeffer, L., Wold, B., 2008. Mapping and quantifying mammalian transcriptomes by RNA-seq. Nat. Methods 5, 621–628. https://doi.org/10.1038/nmeth.1226.

Ni, Z., Tian, X., Zhao, W., Hu, W., Lv, J., Sun, X., Zhang, Y., Zhang, Y., Zhang, Y., Li, B., Liu, F., 2025. The detrimental effects and mechanisms of Orlistat in disrupting energy homeostasis and reproduction in *Daphnia magna*. Aquat. Toxicol. 279. https://doi.org/10.1016/j.aquatox.2024.107201.

Nkoom, M., Lu, G., Liu, J., Dong, H., Yang, H., 2019a. Bioconcentration, behavioral, and biochemical effects of the non-steroidal anti-inflammatory drug diclofenac in *Daphnia magna*. Environ. Sci. Pollut. Res. Int. 26, 5704–5712. https://doi.org/10.1007/s11356-018-04072-3.

Nkoom, M., Lu, G., Liu, J., Yang, H., Dong, H., 2019b. Bioconcentration of the antiepileptic drug carbamazepine and its physiological and biochemical effects on *Daphnia magna*. Ecotoxicol. Environ. Saf. 172, 11–18. https://doi.org/10.1016/j.ecoenv.2019.01.061.

Pal, S., Jana, N.R., 2020. Pharmacologic vitamin C-based cell therapy via iron oxide nanoparticle-induced intracellular fenton reaction. ACS. Appl. Nano Mater. 3, 1683–1692. https://doi.org/10.1021/acsanm.9b02405.

Pan, Y., Yan, S.-w., Li, R.-z., Hu, Y.-w., Chang, X.-x., 2017. Lethal/sublethal responses of *Daphnia magna* to acute norfloxacin contamination and changes in phytoplankton-zooplankton interactions induced by this antibiotic. Sci. Rep. 7. https://doi.org/10.1038/srep40385.

Pham, V.T.H., Vi Khanh, T., Quinn, M.D.J., Notley, S.M., Guo, Y., Baulin, V.A., Al Kobaisi, M., Crawford, R.J., Ivanova, E.P., 2015. Graphene induces formation of pores that kill spherical and rod-shaped bacteria. ACS. Nano 9, 8458–8467. https://doi.org/10.1021/acsnano.5b03368.

Qin, L., Li, R., He, H., Jiang, S., Zhang, P., 2020. Preparation and degradation properties of black phosphorus nanosheets. J. Shenyang Pharma. Univ. 37, 385–389.

Qiu, M., Wang, D., Liang, W.Y., Liu, L.P., Zhang, Y., Chen, X., Sang, D.K., Xing, C.Y., Li, Z. J., Dong, B.Q., Xing, F., Fan, D.Y., Bao, S.Y., Zhang, H., Cao, Y.H., 2018. Novel concept of the smart NIR-light-controlled drug release of black phosphorus nanostructure for cancer therapy. Proc. Natl. Acad. Sci. U.S.A. 115, 501–506. https://doi.org/10.1073/pnas.1714421115.

Smith, L.S., Haidari, H., Amsalu, A., Howarth, G.S., Bryant, S.J., Walia, S., Elbourne, A., Kopecki, Z., 2024. Black phosphorus nanoflakes: an emerging nanomaterial for clinical wound management and biomedical applications. Int. J. Mol. Sci. 25. https://doi.org/10.3390/ijms252312824.

Sun, W.-H., Liu, F., Chen, Y., Zhu, Y.-C., 2012. Hydrogen sulfide decreases the levels of ROS by inhibiting mitochondrial complex IV and increasing SOD activities in cardiomyocytes under ischemia/reperfusion. Biochem. Biophys. Res. Commun. 421, 164–169. https://doi.org/10.1016/j.bbrc.2012.03.121.

Sun, Y., Li, X., Fan, S., Li, C., Shang, Z., Gu, M., Liang, S., Tian, X., 2020. In *vitro* and in *vivo* toxicity of black phosphorus nanosheets. J. Nanosci. Nanotechnol. 20, 659–667. https://doi.org/10.1166/jnn.2020.16922.

Thurakkal, S., Zhang, X., 2020. Recent advances in chemical functionalization of 2D black phosphorous nanosheets. Adv. Sci. 7. https://doi.org/10.1002/advs.201902359.

Tkaczyk, A., Bownik, A., Dudka, J., Kowal, K., Slaska, B., 2021. *Daphnia magna* model in the toxicity assessment of pharmaceuticals: a review. Sci. Tot. Environ. 763. https://doi.org/10.1016/j.scitotenv.2020.143038.

Wang, X., Tan, Z., Chen, S., Gui, L., Li, X., Ke, D., Hou, L., Leung, J.Y.S., 2021. Norethindrone causes cellular and hepatic injury in zebrafish by compromising the

metabolic processes associated with antioxidant defence: insights from metabolomics. Chemosphere 275. https://doi.org/10.1016/j.chemosphere.2021.130049.

Wang, N., Wang, Y., Zhang, R., Sun, A., Lu, Y., Zhang, Z., Shi, X., 2025. Accumulation patterns and chronic toxic effects of triphenyl phosphine in mytilus coruscus. Aquaculture 596. https://doi.org/10.1016/j.aquaculture.2024.741869.

Wang, P., Huang, B., Chen, Z., Lv, X., Qian, W., Zhu, X., Li, B., Wang, Z., Cai, Z., 2019. Behavioural and chronic toxicity of fullerene to *Daphnia magna*: mechanisms revealed by transcriptomic analysis. Environ. Pollut. 255. https://doi.org/10.1016/j.envpol.2019.113181.

Wang, Y., Liu, M., Zang, Y., Zhou, C., Xin, Y., Chai, C., Li, Y., Ma, D., 2022. Ascorbic acid enhanced $MnFe_2O_4$/peroxymonosulfate oxidation of organic pollutant: Key role of singlet oxygen generation and Fe/Mn cycling. J. Environ. Manage. 321. https://doi.org/10.1016/j.jenvman.2022.115971.

Wang, Z., Song, L., Zhang, F., Wang, D.-G., 2020. Comparative acute toxicity and oxidative stress responses in three aquatic species exposed to stannic oxide nanoparticles and stannic chloride. Bull. Environ. Contam. Toxicol. 105, 841–846. https://doi.org/10.1007/s00128-020-03052-z.

Wu, Q., Yao, L., Zhao, X., Zeng, L., Li, P., Yang, X., Zhang, L., Cai, Z., Shi, J., Qu, G., Jiang, G., 2020. Cellular uptake of few-layered black phosphorus and the toxicity to an aquatic unicellular organism. Environ. Sci. Technol. 54, 1583–1592. https://doi.org/10.1021/acs.est.9b05424.

Xiang, Q.-Q., Li, Q.-Q., Wang, P., Yang, H.-C., Fu, Z.-H., Liang, X., Chen, L.-Q., 2024a. Metabolomics reveals the mechanism of persistent toxicity of AgNPs at environmentally relevant concentrations to *Daphnia magna*. Environ. Sci. Nano. https://doi.org/10.1039/d4en00350k.

Xiang, Q., Wang, Z., Yan, J., Niu, M., Long, W., Ju, Z., Chang, X., 2024b. Metabolomic analysis to understand the mechanism of $Ti_3C_2T_x$ (MXene) toxicity in *Daphnia magna*. Aquat. Toxicol. 270. https://doi.org/10.1016/j.aquatox.2024.106904.

Xiong, Z., Zhang, X., Zhang, S., Lei, L., Ma, W., Li, D., Wang, W., Zhao, Q., Xing, B., 2018. Bacterial toxicity of exfoliated black phosphorus nanosheets. Ecotoxicol. Environ. Saf. 161, 507–514. https://doi.org/10.1016/j.ecoenv.2018.06.008.

Xu, D., Liu, J., Wang, Y., Jian, Y., Wu, W., Lv, R., 2020. Black phosphorus nanosheet with high thermal conversion efficiency for photodynamic/photothermal/immunotherapy. ACS. Biomater. Sci. Eng. 6, 4940–4948. https://doi.org/10.1021/acsbiomaterials.0c00984.

Yang, X., Liang, J., Wu, Q., Li, M., Shan, W., Zeng, L., Yao, L., Liang, Y., Wang, C., Gao, J., Guo, Y., Liu, Y., Liu, R., Luo, Q., Zhou, Q., Qu, G., Jiang, G., 2021. Developmental toxicity of few-layered black phosphorus toward *Zebrafish*. Environ. Sci. Technol. 55, 1134–1144. https://doi.org/10.1021/acs.est.0c05724.

Yang, Y., Wang, M., Pan, H., Zhang, R., Wang, L., 2017. Effects of different density of *Daphnia magna* on phytoplankton community. J. Shanghai Ocean Univ. 26, 406–414.

Young, M.D., Wakefield, M.J., Smyth, G.K., Oshlack, A., 2010. Gene ontology analysis for RNA-seq: accounting for selection bias. Genome Biol. 11. https://doi.org/10.1186/gb-2010-11-2-r14.

Yuan, D., Zhang, B., 2025. Assessing the chronic toxicity of climbazole to *Daphnia magna*: physiological, biochemical, molecular, and reproductive perspectives. Comp. Biochem. Physiol. C-Toxicol. Pharmacol. 287. https://doi.org/10.1016/j.cbpc.2024.110061.

Zhang, X.J., Zhang, Z.M., Zhang, S.Y., Li, D.Y., Ma, W., Ma, C.X., Wu, F.C., Zhao, Q., Yan, Q.F., Xing, B.S., 2017. Size effect on the cytotoxicity of layered black phosphorus and underlying mechanisms. Small. 13. https://doi.org/10.1002/smll.201701210.

Zhao, Y., Wu, Z., Dang, Z., Hao, J., 2022. Progress in the synthesis of 2D black phosphorus beyond exfoliation. Appl. Phys. Rev. 9. https://doi.org/10.1063/5.0123810.

Zhou, D., Sun, T., Huang, Y., Chen, X., Shang, J., 2021. Role of nonspherical DLVO and capillary forces in the transport of 2D delaminated Ti3C2Tx MXene in saturated and unsaturated porous media. Environ. Res. 200. https://doi.org/10.1016/j.envres.2021.111451.